Efficient analog multiband channelization for bandwidth scaling in mm-wave systems

H. Roufarshbaf, U. Madhow, M. Rodwell
Department of Electrical and Computer Engineering
University of California, Santa Barbara, CA
Email: {hroufarshbaf, madhow, rodwell}@ece.ucsb.edu

S. Rajagopal
Samsung Research America
Dallas, TX
Email: {sridhar.r}@samsung.com

***Abstract*—We consider analog multiband as a means for scaling up the bandwidth for millimeter (mm) wave communication. Analog multiband sidesteps the difficulty of scaling analog-to-digital conversion (ADC) to higher sampling rates by channelizing the available bandwidth in the analog domain into subbands and using existing power-efficient ADCs to digitize each subband. In this paper, we address the issue of efficient channelization into subbands. A direct approach using a bank of mixers with independent frequency synthesizers has several disadvantages, including large power consumption and the potential for oscillator coupling. We explore an alternative approach based on polyphase sampling, using analog discrete Fourier transform (DFT) along with appropriately designed baseband filters. We quantify the inter-subband interference as a function of filter choice, and demonstrate that it can be handled using interference suppression strategies developed in our prior work. A natural comparison of such approaches, where analog channelization is followed by parallel ADCs running at slower rates for each subband, is with time-interleaved ADCs, which also use polyphase samplers, but use parallel sub-ADCs to digitize the entire band. We show that the proposed approach reduces the required dynamic range of the subband ADCs in comparison to the TI-ADC.**

I. Introduction

Advances in radio frequency integrated circuits (RFICs) are opening up the possibility of commercial utilization of the large amounts of spectrum available at millimeter wave carrier frequencies, including the 7 GHz of unlicensed spectrum at 60 GHz. This gives us the opportunity to scale wireless communication bandwidths to multiples of GHz. However, a key difficulty in realizing such systems using modern "mostly digital" transceiver architectures are the cost and power inefficiency (and often lack of commercial availability) of analog-to-digital conversion (ADC) of sufficient resolution at such high sampling rates. A natural approach to this problem is to parallelize and use multiple ADCs, each working at a lower sampling rate. This parallelization can be performed in the time domain through time interleaving, leading to the time-interleaved ADC (TI-ADC) [1]. In this paper, we investigate an alternative frequency domain approach, with parallel transmission of data over multiple subbands. The key idea is to perform subband channelization in the analog domain, so that ADC and digital signal processing (DSP) can be performed in parallel for each subband at a slower rate. Within a subband, it is possible to use a variety of modulation techniques, including singlecarrier and orthogonal frequency division multiplexing (OFDM) with cyclic prefix (CP). It has been shown in prior work [2], [3] that, even if the subbands overlap, it is possible to effectively handle the inter-subband interference (as well as the intersymbol interference within a subband). In the present paper, we investigate efficient techniques for channelization into subbands. Our performance evaluation is for 60 GHz indoor communication under a channel model developed under the IEE 802.11ad standard, using OFDM with CP over each subband.

Figure 1 depicts the basic concept of analog multiband, with a direct approach to channelization using a bank of mixers, each tuned to the center frequency of one of the subbands. However, implementation of such a mixer bank with independent local oscillators is not power-efficient, and adequate isolation across mixers is a major challenge in circuit design [4]. In this paper, we adapt recently developed ideas in polyphase sampling and mixing [5] for efficient channelization in our context, and evaluate these for an indoor 60 GHz channel model.

Contributions: We investigate frequency domain channelization based on polyphase sampling of the received signal in analog domain. We consider an analog implementation model for filtered multitone modulation (FMT) which can be efficiently implemented using analog IDFT/DFT blocks based on the FFT butterfly structure. We investigate inter-subband interference for FMT when it is operating at its highest spectral efficiency (under a so-called critical condition), and show that, for appropriate choice of filters, excellent performance is obtained without the use of a CP for the overall signal. Within a subband, the channel delay spread (in terms of number of samples) is relatively small because of the slower sampling rate, hence OFDM with a short CP is an efficient means of handling intersymbol interference. While our polyphase sampling rate is comparable to that of a TI-ADC digitizing the entire band, using the analog DFT reduces the peak to average power ration (PAR) prior to digitization, so that the parallel ADCs in our architecture can employ a smaller dynamic range. To get a concrete sense of the channel bandwidths and data rates potentially achievable using such an architecture using the *current* state of the art in ADC technology, we note that 500 MHz corresponds to a knee in the curve of power efficiency versus sampling rate [6] (see the figure on Walden FOM versus speed). Thus, setting the subband size to

978-1-4673-6432-4/15/$31.00

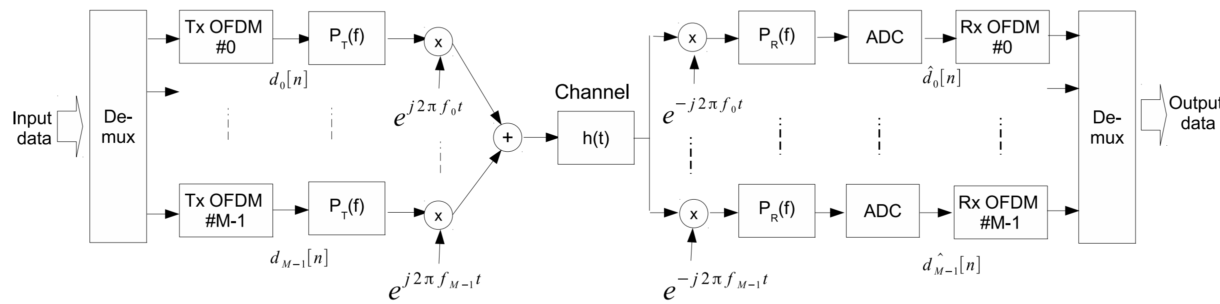

Fig. 1. Analog multiband block diagram for bandwidth scaling at mm-wave through spectrum channelization. Data symbols are demultiplexed into M subbands. Each subband is an OFDM communication block diagram and a mixer banks is used to line up the subband spectrums in frequency domain.

500 MHz, and channelizing using a moderate-sized 16-point analog FFT, we can attain signaling bandwidths of 8 GHz, more than enough, for example, to cover the entire 7 GHz of unlicensed spectrum at 60 GHz. Coupling this with a power-efficient constellation such as 16QAM, together with 4-fold spatial/polarimetric multiplexing, we see the potential for data rates in excess of 100 Gbps.

Related work: Parallel channelization of the spectrum for mm-wave communication systems is also addressed in [7]. Their approach in channelization is based on sub-harmonic mixing at the transceivers which suffers from varying mixer conversion gain across the channels and require high precision ADCs. Analog DFT for reducing the required ADC dynamic range is proposed for ultra-wideband communication in [8], but it incurs inefficiency due to insertion of a cyclic prefix. The FMT approach proposed here is similar to a channelization approach for optical communication systems in [9]. However, the latter considers a fully digitized received signal through a very high-speed ADC, whereas we reduce dynamic range via analog DFT prior to digitization. Our performance evaluation model is also different because of our focus on the indoor mm-wave channel.

We first review the proposed multiband communication scheme for mm-wave channel (Section II). The FMT channelizer technique based on polyphase sampling is discussed in Section III. Numerical performance analysis and conclusions are presented in Sections V and VI, respectively.

II. Multiband communication structure

Figure 1 shows the basic analog multiband concept. The input data sequence is demultiplexed into M parallel subbands. Each subband is an OFDM communication block which modulates the data sequence into N subcarriers, performs data interleaving and channel encoding, and delivers the modulated data to the transmit filter $p_T(t)$ for pulse shaping. The pulse-shaped signals of the parallel subbands are piled up on top of each other in the frequency domain to cover the total bandwidth of the mm-wave communication system. At the receiving side, each subband signal is separated out using analog processing prior to digitization. The ADCs used for the latter purpose can therefore run at speeds dictated by the subband bandwidth, which are much lower than those required to digitize the entire spectrum used. The digitized signal is used for further signal processing including standard OFDM processing and inter-subband interference suppression.

We now provide a mathematical description of the preceding system blocks, and discuss the design requirements. Denote OFDM samples of subband k by $d_k[n]$ where k, $k = 0, \cdots, M-1$. The OFDM sample rate within the subband is $1/T$. The transmit signal is an aggregate of the pulse-shaped/frequency-shifted subband signals and is given by

$$x(t) = \sum_n \sum_{k=0}^{M-1} d_k[n] p_T(t-nT) e^{j2\pi(t-nT)f_k} \quad (1)$$

$$= \sum_n \sum_{k=0}^{M-1} d_k[n] p_{T,k}(t-nT), \quad (2)$$

where $p_{T,k}(t-nT)$ is defined as $p_{T,k}(t) = p_T(t)e^{j2\pi t f_k}$. In an ideal channel, the received signal is equal to the transmitted signal. The transmitted OFDM samples on each subband can be reconstructed when [10]

$$\int_{-\infty}^{\infty} p_{T,k}(t-mT) p^*_{R,l}(t-nT) dt = \delta_{kl}\delta_{mn}, \quad (3)$$

where δ is the Kronecker delta function. A simple pulse shaping signal which satisfies (3) is a rectangular pulse with time duration T. Other forms of the pulse shaping signals are the raised-cosine and the square root raised cosine filters.

Channel time dispersion causes both intersymbol interference within a subband (handled in our setting via OFDM with CP) and inter-subband interference. In the presence of a time dispersive channel, one can calculate the equivalent channel from each transmit subband to a specific receive subband and characterize the resulting interference at the OFDM subcarrier level [3]. While we leverage these results in our performance evaluation, our main interest here is in channelization techniques that are more efficient than the mixers bank shown in Figure 1.

III. Filtered Multitone (FMT) Channelization

We now discuss an alternative approach to channelization that avoids the use of a mixer bank as in Figure 1. As

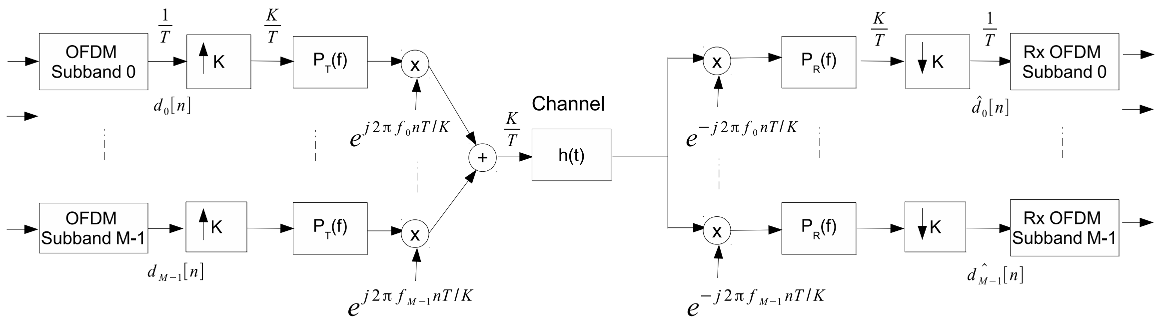

Fig. 2. The FMT channelizer scheme with OFDM subbands.

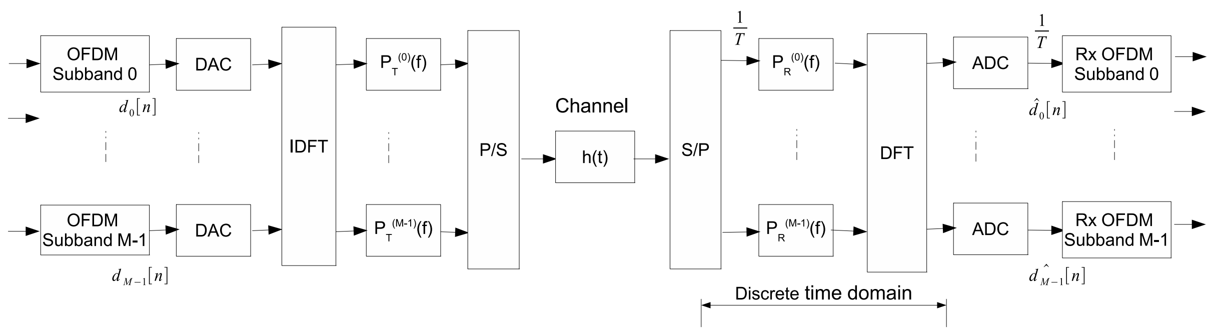

Fig. 3. The proposed FMT channelizer in the critical condition ($K = M$ in comparison to Figure 2) with IDFT/FFT at the discrete time domain (analog IDFT/DFT).

mentioned earlier, that implementation of a mixers bank (Figure 1) is not an efficient way to implement the analog multiband channelizer. We base our approach on the analog DFT, which is attractive since, for a number of subbands equal to a power of 2, the IDFT/DFT can be efficiently implemented using the butterfly structure [8]. Since this is analogous to OFDM, maintenance of orthogonality requires a cyclic prefix. However, we wish to avoid this, since, for our application, using a cyclic prefix with a moderate sized FFT (with length equal to the number of sub bands) would be prohibitive in terms of overhead: the results of our previous work on indoor mm-wave channels [3] shows that the channel delay spread can be as large as 20 ns even after beamforming, which corresponds to a delay spread of 100 symbols if we are signaling at 5 Gsymbols/sec, for example. We therefore seek an approach for subband channelization that exploits the efficiency of implementing an analog DFT while avoiding CP insertion. We adapt for this purpose filtered multitone (FMT) modulation [11], first introduced for very high speed digital subscriber line (VDSL).

The general structure is depicted in Figure 2. A key difference from the basic analog multiband structure in Figure 1 is the upsampling step. The bandwidth of the transmit signal in each subband is approximately $1/T$. As the signal is upsampled by the factor K, where $K \geq M$ (M is the number of subbands), the spectrum of the output signal is formed in a way that the distance between the adjacent subbands is $\frac{K}{TM}$ (so that the center frequency for subband m is $f_m = mK/TM$). The ratio K/M determines the guardband between the subbands, which becomes zero for the special case $K = M$, termed the "critical condition" in [11]. Since we are interested in maximizing spectral efficiency, we operate in the latter regime, setting $K = M$, handling the spectral leakage across subbands using interference suppression.

At time kT/M, the transmitted signal is given by [11]

$$x(k\frac{T}{M}) = \sum_{m=0}^{M-1}\sum_{n=-\infty}^{\infty} d_m[n] p_T\left[(k-nM)\frac{T}{M}\right] e^{j2\pi mk/M}. \tag{4}$$

By changing the order of summation and applying the change of variable $kT/M = lT + i(T/M)$ where $i = 0, 1, \cdots, M-1$, the output signal is given by

$$x(lT + i\frac{T}{M}) = \sum_{n=-\infty}^{\infty}\left(\sum_{m=0}^{M-1} d_m(nT) e^{j2\pi mi/M}\right) p_T[(l-n)T + i\frac{T}{M}]. \tag{5}$$

The inner summation in (5) is the IDFT of the subband symbols, and the term $p_T[(l-n)T + i\frac{T}{M}]$ is the ith polyphase component of the transmit filter. This suggests that the transmitter block diagram can be modified to perform the IDFT at the first step, then applying the pulse shaping filter on each output of the IDFT block followed by a serial to parallel conversion to order the transmit symbols. The modified transmitter block diagram is shown in Figure 3.

At the receiving side of the FMT block diagram (Figure 2), the signal for subband i is given by

$$\hat{d}_i(nT) = \sum_{k=-\infty}^{\infty} y(k\frac{T}{M})e^{-j2\pi f_i kT/M} p_R(k\frac{T}{M} - nT). \quad (6)$$

Letting $kT/M = lT + mT/M$ and $m = 0, \cdots, M-1$ which models polyphase sampling of the received signal, the sum in (6) can be break down into two summations as follows

$$\hat{d}_i(nT) = \sum_{m=0}^{M-1} \left(\sum_{l=-\infty}^{\infty} y(lT + m\frac{T}{M}) \right. \quad (7)$$
$$\left. p_R[(n-l)T - m\frac{T}{M}] \right) e^{-j2\pi mi/M}.$$

The preceding equation suggests modifying the receiver block diagram based on polyphase sampling as shown in Figure 3, with polyphase samples filtered with the pulse shaping filters corresponding to different subbands, and then performing subband separation via the DFT block.

Discussion: After its original introduction for VDSL [11], this approach has been recently revisited for uplink wireless communication [10], in order to alleviate synchronization requirements for OFDMA as well as for wavelength division multiplexing (WDM) in optical communication systems [9] to remove the requirement for CP insertion at the channelizer level. However, in all of these applications, the ADC is applied at the first step, prior to serial-to-parallel conversion, and subband separation is performed purely digitally. However, given the difficulty of scaling ADC to large bandwidths, we observe here that analog DFT prior to ADC can lead to significant advantages. As we discuss in the next section, this leads to reduction in the peak to average power ratio seen by the ADC, which relieves dynamic range requirements. This is a key advantage over a TI-ADC digitizing the entire band. Furthermore, since the ADCs digitizing different subbands operate independently, at a relatively slow rate and relatively small dynamic range, it becomes possible to employ off-the-shelf ADC technology even as communication bandwidths scale up. Again, this is in contrast to TI-ADC designs where the sub-ADCs running in parallel must be tightly synchronized. Of course, we have not completely eliminated the difficulties of bandwidth scaling, but moving them to the analog domain implies that we can leverage recent advances in efficient implementations of IDFT and DFT [8].

IV. Peak to Average Power Ratio

FMT channelization is efficient because of its utilization of IDFT/DFT. Of course, just as in OFDM, the IDFT stage increases the peak-to-average power ratio (PAR) of the transmitted signal. This increased dynamic range makes direct digitization at the receiver less attractive. We provide numerical

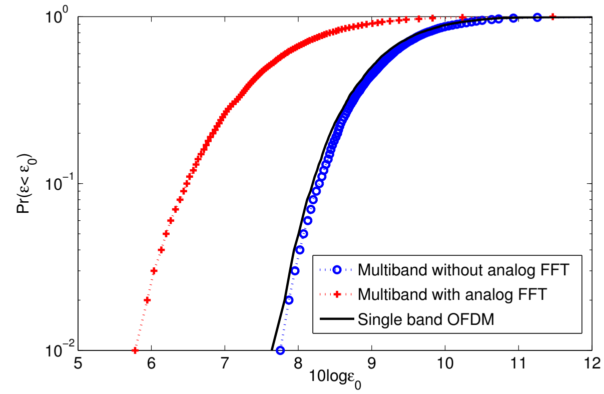

Fig. 4. Empirical distribution of the PAR for a multiband scenario with $M = 16$ OFDM subbands, each contains $N = 64$ subcarriers.

results in this section that show the significant decrease in dynamic range requirements after the analog DFT, even though the channelization/dechannelization is not perfect.

For signal $x(t)$, the signal PAR is defined by

$$\epsilon_0 = \frac{\max |x(t)|^2}{E\{|x(t)|^2\}}, \quad (8)$$

where $E\{\}$ denotes the expectation operation. For the system in Figure 3, the PAR for the OFDM samples of each subband with N subcarriers is $10\log(N)dB$ [12]. By applying the IDFT for channelization of M subbands, the PAR increases by $10\log(M)dB$. This is equivalent to transmitting one single carrier OFDM with MN subcarriers. In time-interleaved ADC structure, lower rate parallel ADCs are located after the polyphase sampler block. Therefore, the PAR seen by each the low rate ADC is equal to the PAR of the received signal. However, considering an ideal channel, if the DFT is performed in the analog domain before the subband ADCs, the PAR of the de-channelized signals prior to the low rate ADCs is equal to that of the transmitted OFDM samples on each subbands ($10\log(N)dB$).

Figure 4 shows the empirical distribution of the PAR for three different scenarios. The distribution is derived when $M = 16$ subbands is simulated and each subband carries the OFDM sample with $N = 64$ subcarriers. In the first scenario, the low rate ADCs are located after the S/P block and the DFT is handled in digital domain. The second scenario is the proposed model which implements analog DFT for de-channelization (Figure 3) and the PAR distribution is derived after analog DFT block. The third scenario shows a single carrier OFDM with $M \times N$ subcarriers (same capacity as M parallel OFDMs with N subcarrier). This can represent the applications of the TI-ADC at the front side of the receiver. As we observe, by applying the DFT de-channelizer in the analog domain, the maximum PAR that is seen by the low rate ADCs is reduced.

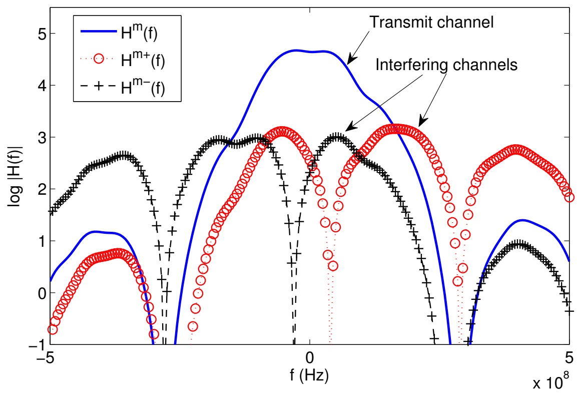

Fig. 5. The frequency response of the subband transmit channel and the adjacent interfering channels when the rectangular filter is implemented.

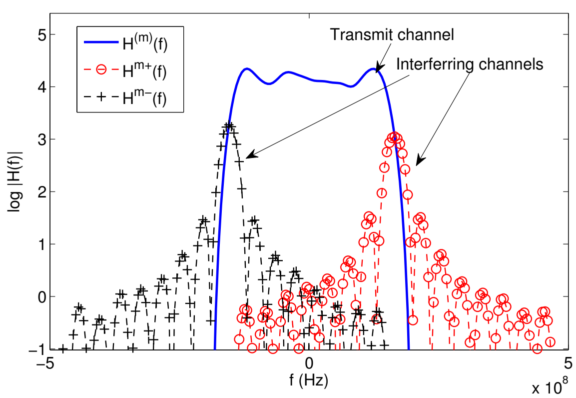

Fig. 6. The frequency response of the subband transmit channel and the adjacent interfering channels when the SRRC filter is implemented.

V. Numerical Analysis

The performance of the proposed channelizer scheme (in the "critical condition" $K = M$) is evaluated using simulations. We consider the conference room scenario of the mm-wave indoor channel standard [13]. The transmitter and receiver each use a 4×4 phased array for beamforming. As in [3], we assume that the beam is formed towards the dominant path (issues of beam adaptation, or optimizing the beam in a more sophisticated fashion, are not addressed). The total bandwidth is set to 4GHz, divided into 16 subbands of size 250 MHz each. Each subband transmits an OFDM signal with 64 subcarriers and CP length of 16. The modulation per subcarrier is 16QAM. Error correcting codes are not included in our simulation, but we note that an uncoded BER of 10^{-2} or smaller is easily handled by lightweight coding. We first evaluate the effect of the transmit and receive filter type on inter-subband interference.

A. *Inter-subband interference*

To evaluate the inter-subband interference, we consider the communication model in Figure 2. The equivalent channel in frequency domain from transmit subband i to the receive subband k is given by

$$H_{eq}^{i,k}(f) = P_T(f - f_i)H(f)P_R(f - f_k). \tag{9}$$

For $i = k$, the equivalent channel shows the transmit channel and for $i \neq k$, the equivalent channel shows the interference channels (ICI). Figures 5 and 6 show the frequency response of the equivalent transmit and interfering channels based on various selections of the subband filter ($P_T(f)$). $H^m(f)$ shows the transmit channel for subband m, and $H^{m-}(f)$ and $H^{m+}(f)$ shows the interfering channels from adjacent subbands $m-1$ and $m+1$, respectively. In Figure 5, we observe that the leakage from the interfering channels is widespread over the entire transmit band. This is due to sharp variation in the time domain signal, which generates large sidelobes. When square root raised cosine (SRRC) with roll-off factor $\alpha = 0.125$ is chosen (Figure 6), the inter-subband interference is only limited to the boundaries of the transmit band.

Figure 7 compares the BER per OFDM subcarrier of the transmit channel when the rectangular pulse filter are selected with the scenario that the SRRC filters are selected. The SNR is fixed to 40 dB and no interference suppression technique is applied. Hence, the error rate is due to the interference rather than the additive Gaussian noise. We see that when the rectangular pulse is used, the interference is spread over the entire subband, and affects all subcarriers. (Of course, the subcarriers in the middle still see lower interference than at the edges). Using the SRRC pulse at the transmit and the receive side, the interference is only significant at the boundary subcarriers.

Given that interference at a given subband is dominated by its neighboring subbands, it suffices to restrict attention to a single subband in the presence of interference from its two neighbors. Simulation results on the performance of the FMT channelization technique are presented in Figure 8. We consider the interference model derived in our prior work [3] which states that each subcarrier of the subband OFDM symbols only sees interference from the same subcarrier number in the adjacent subbands. Considering this model, joint detection for each subcarrier number across the subbands is applied. For interference suppression, the MMSE linear equalizer (trained over 25 OFDM symbols) is implemented. As we can observe from Figure 8, the FMT scheme with SRRC filter performs similar to our previous work [3], which assumes a bank of mixers. This shows that the specific interference model that is previously derived is valid when SRRC multirate filters are used. However, when rectangular filter is used, the performance even with the MMSE equalizer is worse than the SRRC filter without interference suppression. This is because the orthogonality between the OFDM subcarriers within the subband and across subbands no longer holds, with every subcarrier is interfering with other subcarriers of the adjacent subband. Therefore, a more complicated interference model must be used to improve the performance if rectangular filters are used.

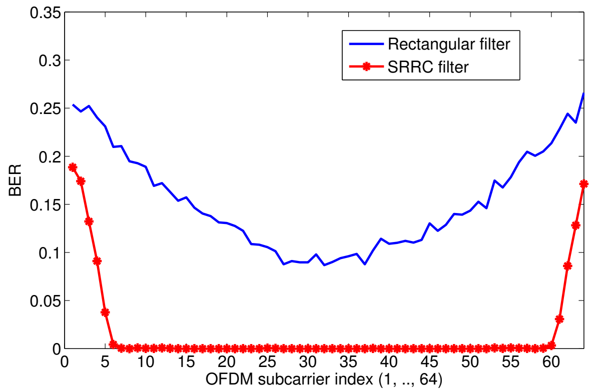

Fig. 7. BER per OFDM subcarrier of the transmit channel when rectangular filters or SRRC filters are applied.

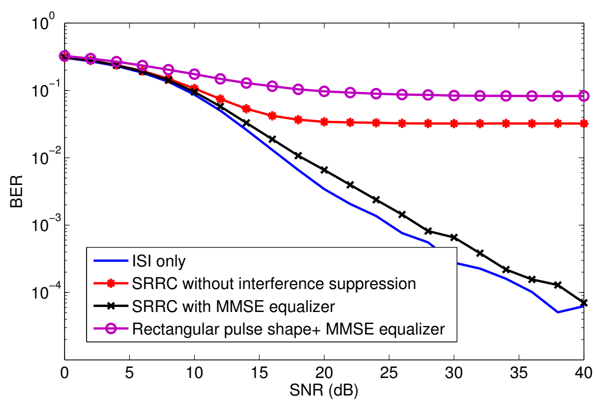

Fig. 8. BER v.s. SNR for the proposed channelizing structure in mm-wave conference room scenario.

VI. Conclusions

Prior work has shown that analog multiband is an attractive approach for scaling up communication bandwidths while using off-the-shelf ADCs, and that high spectral efficiency can be attained by using linear interference suppression techniques to mitigate inter-subband interference. In this paper, we explore efficient techniques for channelization into subbands using polyphase samplers and linear analog operations, rather than a bank of mixers. De-channelizing in the analog domain, as is performed in the modified FMT channelizer, reduces the maximum PAR of the subband signal, thus simplifying the task of digitization. While we have considered OFDM within a subband, the PAR could be reduced further by use of singlecarrier modulation on the subbands.

At the receiver, our approach to channelization involves sampling at full rate, then some linear operations, and then parallel digitization of the subband signals. This invites a natural comparison to TI-ADCs for digitizing the entire band using a number of parallel sub-ADCs. As we have discussed earlier, our architecture has advantages in terms of reduced dynamic range for the parallel ADCs and the ability of these ADCs to operate independently, rather than in tightly synchronized fashion as in a TI-ADC. However, an important problem for further investigation is the sensitivity of our channelization strategies to timing and gain mismatch at the full-rate sampling stage. This is analogous to mismatches across sub-ADCs for a TI-ADC, which have received significant attention in the literature, including the development of frameworks for joint channel and mismatch compensation [14]. It is of great interest to develop analogous models and compensation strategies to our polyphase sampler/mixer architectures. Another important class of problems for future work is to explore the tight integration of analog multiband with spatial techniques, including diversity and multiplexing as well as beamforming.

Acknowledgment

This research was supported in part by Samsung Research America - Dallas. We acknowledge the help and feedback from researchers in Samsung Research America - Dallas on this work.

References

[1] M. El-Chammas and B. Murmann, *Background Calibration of Time-Interleaved Data Converters*. Analog Circuits and Signal Processing, 2012.

[2] H. Zhang, S. Venkateswaran, and U. Madhow, "Analog multitone with interference suppression: Relieving the ADC bottleneck for wideband 60 GHz systems," in *IEEE GLOBECOM*, March 2012, pp. 2305–2310.

[3] H. Roufarshbaf, U. Madhow, and S. Rajagopal, "OFDM-based analog multiband: A scalable design for indoor mm-wave wireless communication," in *IEEE GLOBECOM*, Dec 2014, pp. 3267–3272.

[4] T. Forbes, W. G. Ho, and R. Gharpurey, "Design and analysis of harmonic rejection mixers with programmable LO frequency," *IEEE Journal of Solid-State Circuits*, vol. 48, no. 10, pp. 2363–2374, October 2013.

[5] C. Andrews and A. C. Molnar, "A passive mixer-first receiver with digitally controlled and widely tunable RF interface," *IEEE Journal of Solid State Circuits*, vol. 45, no. 12, pp. 2696 – 2708, December 2010.

[6] B. Murmann. ADC performance survey 1997-2014. [Online]. Available: http://www.stanford.edu/∼murmann/adcsurvey.html.

[7] V. Dyadyuk, J. D. Bunton, J. Pathikulangara, R. Kendall, O. Sevimli, L. Stokes, and D. A. Abbott, "A multigigabit millimeter-wave communication system with improved spectral efficiency," *IEEE Transactions on Microwave Theory and Techniques*, vol. 55, no. 12, pp. 2813–2821, December 2007.

[8] M. Lehne and S. Raman, "A discrete-time FFT processor for ultra-wideband OFDM wireless transceivers: Architecture and behavioral modeling," *IEEE Transactions on Circuits and Systems*, vol. 57, no. 11, pp. 3011–3022, November 2010.

[9] A. Tolmachev and M. Nazarathy, "Filter-bank based efficient transmission of reduced-guard-interval OFDM," *Optics Express B370*, vol. 19, no. 26, December 2011.

[10] B. Farhang-Boroujeny, "OFDM versus filter bank multicarrier," *IEEE Signal Processing Magazine*, vol. 28, no. 3, pp. 92–112, May 2011.

[11] G. Cherubini, E. Eleftheriou, and S. Olcer, "Filtered multitone modulation for very high-speed digital subscriber lines," *IEEE transactions on Selected Area in Communications*, vol. 20, no. 5, pp. 1016–1028, June 2002.

[12] A. D. S. Jayalath and C. R. N. Athaudage, "On the PAR reduction of OFDM signals using multiple signal representation," in *IEEE International Symposium on Personal, Indoor and Mobile Radio Communication*, September 2003, pp. 799–803.

[13] "Channel models for 60 GHz WLAN systems," *IEEE 802.11-09/0334r8*, 2010.

[14] P. Sandeep, U. Madhow, M. Seo, and M. Rodwell, "Joint channel and mismatch correction for OFDM reception with time-interleaved ADCs: towards mostly digital multiGigabit transceiver architectures," in *IEEE GLOBECOM*, November 2008, pp. 1–5.